SCIENTIFIC REPORTS

OPEN

SUBJECT AREAS:
SURFACES, INTERFACES AND THIN FILMS
MECHANICAL AND STRUCTURAL PROPERTIES AND DEVICES
MOLECULAR MACHINES AND MOTORS
CARBON NANOTUBES AND FULLERENES

Received
27 June 2012

Accepted
29 October 2012

Published
20 December 2012

Correspondence and requests for materials should be addressed to A.V.S. (asavin@center.chph.ras.ru)

Transport of fullerene molecules along graphene nanoribbons

Alexander V. Savin[1,2] & Yuri S. Kivshar[2]

[1]Semenov Institute of Chemical Physics, Russian Academy of Sciences, Moscow 119991, Russia, [2]Nonlinear Physics Center, Research School of Physics and Engineering, Australian National University, Canberra ACT 0200, Australia.

We study the motion of C_{60} fullerene molecules and short-length carbon nanotubes on graphene nanoribbons. We reveal that the character of the motion of C_{60} depends on temperature: for $T < 150$ K the main type of motion is sliding along the surface, but for higher temperatures the sliding is replaced by rocking and rolling. Modeling of the buckyball with an included metal ion demonstrates that this molecular complex undergoes a rolling motion along the nanoribbon with the constant velocity under the action of a constant electric field. The similar effect is observed in the presence of the heat gradient applied to the nanoribbon, but mobility of carbon structures in this case depends largely on their size and symmetry, such that larger and more asymmetric structures demonstrate much lower mobility. Our results suggest that both electorphoresis and thermophoresis can be employed to control the motion of carbon molecules and fullerenes.

Over the past 20 years nanotechnology has made an impressive impact on the development of many fields of physics, chemistry, medicine, and nanoscale engineering[1]. After the discovery of graphene as a novel material for nanotechnology[2], many properties of this two-dimensional object have been studied both theoretically and experimentally[3,4]. In addition to its unusual properties, graphene may play an important role as a component of more complex systems of nanotechnology. In particular, atoms or molecules deposited on a surface of single-layer graphene[5] are expected to move with just two degrees of freedom, demonstrating various phenomena that can be employed for nanomechanics and nanoscale molecular motors[6].

Numerical modeling of the motion of atoms and molecules on a graphene sheet was considered very recently in a number of studies[7–9]. In the first approximation, one may treat graphene as a planar two-dimensional substrate that creates an effective two-dimensional periodic potential for absorbed molecules. Stochastic motion of noble gases on such a substrate potential was analyzed in Ref. 7. It was shown that Xe atom is trapped in a potential well of the substrate at high friction while He atom can freely diffuse. Diffusive motion of C_{60} molecules on a graphene sheet was modeled in Ref. 8. Analytical and numerical studies demonstrated that the translation motion of C_{60} molecule near a graphene sheet is diffusive in the lateral direction, whereas in the perpendicular direction this motion can be described as diffusion in an effective harmonic potential (bounded diffusion). It was also shown that the motion of C_{60} over graphene sheet is not rolling. More detailed analysis of the structure of the effective two-dimensional periodic potential for C_{60} molecules was carried out in Ref. 9. It was shown that the energetically favorable motion of fullerene molecules is sliding along the surface when one side of the C_{60} molecule remains parallel to the plane of the graphene and the molecule center is placed above the valent bond of the nanoribbon. However, all those results were obtained for the case when the graphene nanoribbon is assumed to be flat and rigid, so that the motion of its atoms is not taken into account.

Directed motion of C_{60} molecules along the graphene sheet under the action of a heat flow was studied numerically in Ref. 10. In their calculations, the authors employed the so-called Nosé-Hoover thermostat, which however is known to produce incorrect results in the nonequilibrium molecular dynamics simulations[11,12]. In addition, the directed motion of the fullerenes were not analyzed.

By now, novel nanocomposite structures consisting of a stacked single graphene sheet and C_{60} monolayer were produced experimentally[13]. It was found that the intercalated C_{60} molecules can rotate in between graphene sheets. Such a rotation of a single C_{60} molecule on a sheet of graphene should result into its rocking and rolling motion, in contrast to the statement of Ref. 8. In order to resolve those controversies and model more general dynamics closely resembling the experimental conditions, one have to take into account the motion of carbon atoms of the nanoribbon that will modify its planar geometry due to the interaction with C_{60} fullerene molecules.

In this paper, we study numerically different types of motion of carbon structures, such as C_{60} fullerene molecules and short-length carbon nanotubes, on finite-width graphene nanoribbons. We employ molecular

dynamics simulations taking into account the motion of all carbon atoms, and demonstrate that an edge of the nanoribbon creates a potential barrier for the absorbed nanostructures supporting their transport along the nanoribbon. We study different types of dynamics including stochastic Brownian like motion as well as directed motion of fullerenes driven by the electric field and temperature gradient. We reveal that the motion of C_{60} fullerene molecules depends on the temperature, so that for low temperatures the main type of motion is sliding along the surface, but for higher temperatures the sliding is replaced by rocking and rolling. For the directed motion, the mobility depends largely on the shape and symmetry of the carbon structures, so that larger and asymmetric structures demonstrate much lower mobility. Our results suggest that both electorphoresis and thermophoresis can be employed to control and direct carbon structures and fullerenes.

Results

Detailed modeling of the motion of a C_{60} molecule inside a single-walled carbon nanotube was carried out in a series of studies[14–17]. In particular, Ref. 14 studied the motion of C_{60} inside (11,11) SWNT (the system C_{60}@SWNT), Ref. 15 analyzed the oscillatory motion between the edges of a finite-length (10,10) SWNT, and Ref. 16 demonstrated that the energy dissipation of the oscillatory motion of C_{60} depends substantially on the radius of SWNT and the presence of defects. Thermophoretic motion of buckyball enclosed in a series SWNTs was analyzed in Ref. 17. It was shown that inside the nanotube the encapsulated fullerenes move in the direction opposing the thermal gradient, i.e. in the direction of the thermal flow. Similar behavior of the C_{60} molecule was predicted for a graphene sheet where the fullerenes was shown to move in the direction of a heat flow[10].

In this paper, we study the dynamics of a molecular system consisting of a fullerene molecule C_{60} or short-length carbon nanotubes placed on a graphene nanoribbon, as shown in Figs. 1(a–d). We employ numerical moleculardynamics simulations taking into account the motion of all carbon atoms.

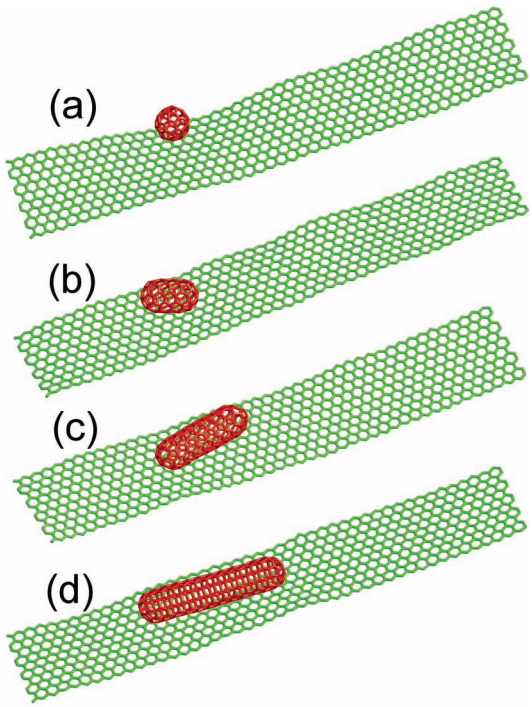

Figure 1 | Motion of (a) fullerene C_{60} molecule, and (b–d) shot-length (5,5) carbon nanotubes C_{100}, (c) C_{180}, and (d) C_{260}, respectively, along a finite-width zigzag carbon nanoribbon. Valent bonds of the nanoribbon are shown in green, while the valent bonds of the absorbed fullerene-like molecules, are shown in red. Temperature is $T = 300$ K.

Approximation of rigid molecules. First, we study the energy of the coupled system "C_{60} + nanoribbon" as a function of the relative position of the buckyball on the surface. We consider a square sheet of graphene of the size 4.1 × 4.1 nm^2 [see Fig. 2 (a)] and

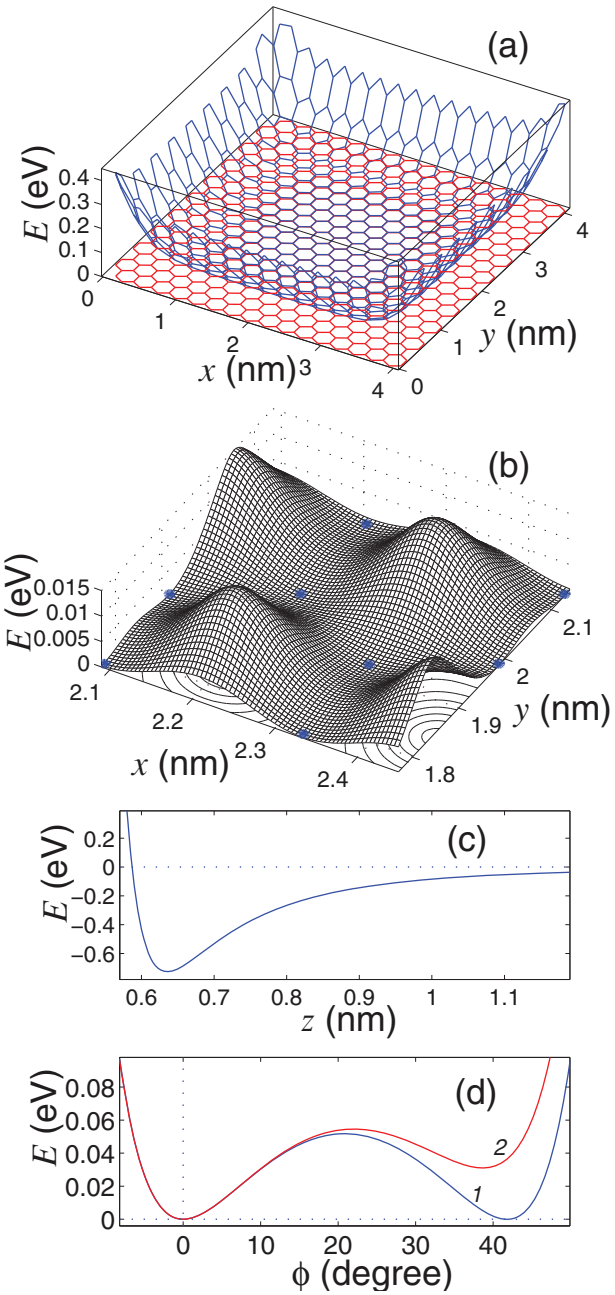

Figure 2 | (a) Energy E of the fullerene C_{60} molecule as a function of its position on a square sheet of a single-layer graphene of the size 4.1 × 4.1 nm^2. Red lines mark the valent bonds of the graphene, where the point (x, y) defines the projection of the molecule center on the plane. (b) Shape of the potential energy $E(x, y)$ at the center of the graphene sheet, circles mark the position of the carbon atoms of the graphene. (c) Interaction energy as a function of the distance z between the center of C_{60} molecule and the plane of graphene. (d) Change the energy of C_{60} molecule due its rotation around the edge closest to the graphene sheet (curve 1: rotation from one hexagon face to the neighboring hexagon face; curve 2: rotation from the hexagon face to the neighboring pentagon face).

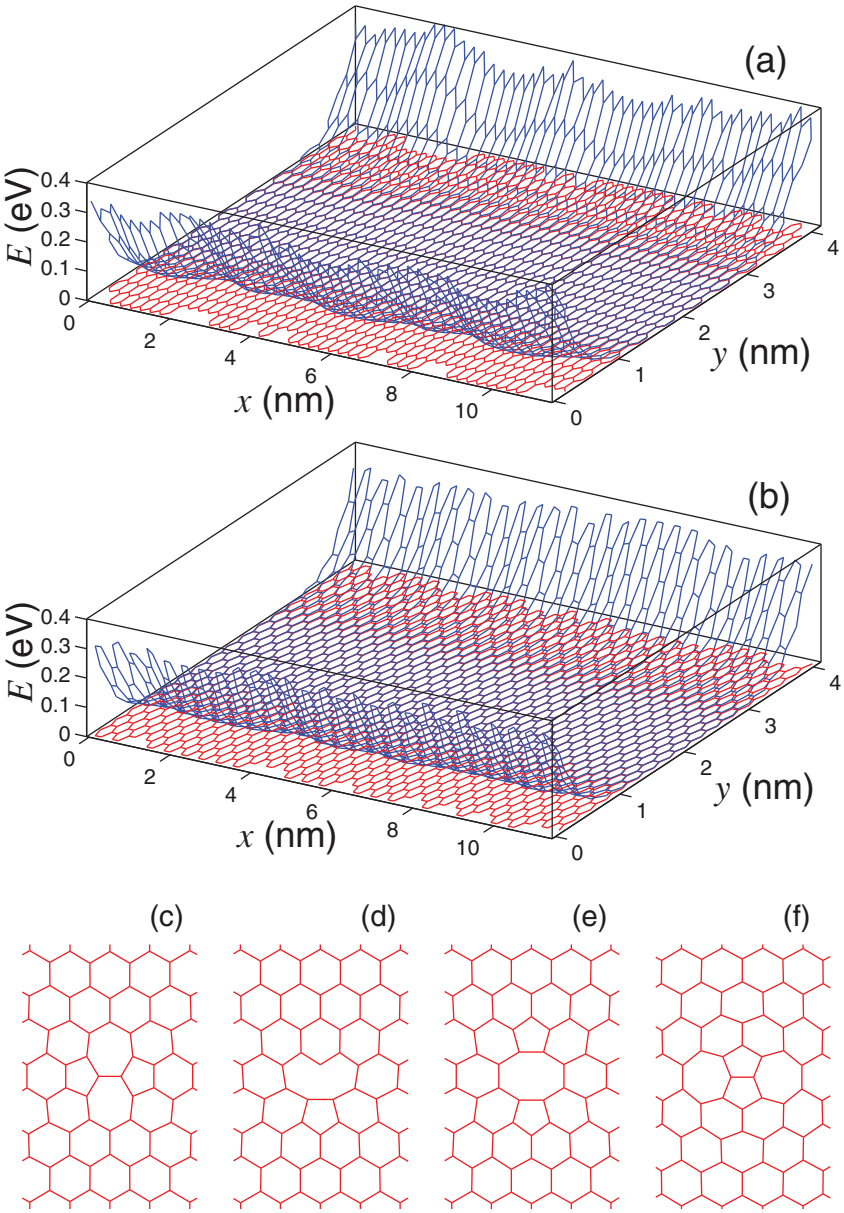

Figure 3 | Energy *E* of the fullerene C_{60} molecule as a function of its position on (a) zigzag and (b) armchair nanoribbons with rough edges. Types of the internal defects of the nanoribbon: (c) Stone-Wales defect (SW), (d) Single vacancy (V_1), (e) Double vacancy defect V_2 and (f) two close carbon adatoms (A_2).

assume that both the C_{60} molecule and the graphene are in the ground state and all valent bonds are not stretched, and the angles between the bonds do not deform. Then the energy of the complex is defined by a sum of all nonvalent interactions (5) between the carbon atoms of the fullerene molecule and the graphene substrate.

Without restrictions of generality, we assume that the sheet of graphene remains at rest in the (x, y) plane, so that the position of the C_{60} molecule is defined by the coordinate (x, y) of its center on the plane and the distance z from the center to the substrate surface. We fix the center coordinate (x, y) and minimize the energy E of the whole molecular complex as a function of the distance z and all angles that define the orientation of the C_{60} molecule in space. Then we obtain two-dimensional function $E(x, y)$ that describes a change of the energy of the system when the fullerene molecule changes its position on the graphene sheet.

The effective potential energy $E(x, y)$ shows that in the ground state the C_{60} molecule takes the position above the center atom of the graphene sheet at the distance $z_0 = 0.635$ nm from the surface, so that the hexagonal face closest to the surface is parallel to it. Figure 2 (c) shows the dependence of the energy E on the distance z to the surface. As follows from this dependence, in order to escape the surface the molecule requires the energy $\Delta E_0 = 0.73$ eV. In the earlier study[8], similar values were defined as $z_0 = 0.65$ nm and $\Delta E_0 = 0.76$ eV, and the experimental evaluation of the coupling energy[18] gave the value $\Delta E_0 = 0.85$ eV.

Dependence of the energy E of the coupled molecular systems on the position coordinate (x, y) of the molecule center on the plane of the graphene sheet is shown in Figs. 2 (a,b). At the center of the sheet, the energy depends on the position of the fullerene molecule, and the positions above the carbon atoms of the substrate are more favorable and they correspond to local minima. The energy profile suggests that the molecule may slide along the graphene sheet with its hexagonal face parallel to the surface following the structure defined by the valent bonds of the substrate. This motion would require overtaking the energy barrier $\Delta E_1 = 0.0015$ eV, whereas the sliding motion in other directions

would require higher energy to overtake the barrier $\Delta E_2 = 0.015$ eV. We notice that the sliding of the C_{60} molecule between two parallel sheets of graphene was studied earlier in Ref. 9, where was found that the corresponding barriers are: $\Delta E_1 = 0.002$ eV and $\Delta E_2 = 0.02$ eV.

When the molecule approaches the edge of the nanoribbon, the total energy of the system $E(x, y)$ grows, as shown in Fig. 2 (a), and at the edge of the nanoribbon potential barrier $\Delta E_3 > 0.3$ eV repels the molecule from the edge.

In addition to the sliding, the C_{60} molecule may also roll along the surface. To evaluate when this rolling becomes possible, we analyze a change of the energy of the ground state when the molecule rotates around the edge of its hexagonal face closest to the graphene surface.

In the ground state the hexagonal face of the fullerene closest to the graphene sheet is parallel to the substrate surface. If we fix one edge of this face and rotate the buckyball around it modeling the rocking of the C_{60} molecule, we can find the dependence of the energy E on the rotation angle ϕ, shown in Fig. 2 (d). For such a procedure, two cases are possible. In the first case, the molecule rotates replacing one hexagonal face by another similar face, the energy $E(\phi)$ for this rotation has the form of a symmetric two-well potential, as shown in Fig. 2 (d, curve 1). For the other type of rotation, the hexagonal face is replaced by a pentagonal face also parallel to the substrate surface, in this later case the energy has the form of asymmetric two-well potential also shown in Fig. 2 (d, curve 2). In both these cases of the molecule rolling, the molecule should overtake the energy barrier $\Delta E_4 = 0.052$ eV substantially higher than the energy barrier ΔE_2 required for its sliding.

For completeness, we also consider the interaction of the C_{60} molecule with defects that may appear in a graphene nanoribbon. Figures 3 (a,b) show the profile of the interaction energy $E(x, y)$ of the molecule for the zigzag and armchair nanoribbons with rough edges. As follows from these results, the presence of defect at the edges does not chance dramatically the shape of the effective potential at the edges but add some distortion and modulation. The main effect, namely the repulsion of the C_{60} molecule from the edges of the nanoribbon remain the same and, therefore, the edge roughness should not change substantially the dynamics of the fullerene inside the ribbon, as was suggested by additional numerical simulations.

To analyze the effect of internal defects on the motion of the fullerene, first we find stationary states with the lowest energy of the four types of defects, namely Stone-Wales defect (SW), Single vacancy (V_1), Double vacancy (V_2) and two close carbon adatoms (A_2), as shown in Figs. 3 (c,d,e,f), respectively. Our numerical simulations reveal that the C_{60} molecule can create bound states with the defects SW, V_1 and V_2 with the binding energies of 0.0039, 0.0024 and 0.0037 eV, respectively. As for the A_2 defect, the interaction of the fullerene molecule with this defect depend on its position above or below the nanoribbon since this defect changes the flat surface of the nanoribbon creating a hump, so that the interaction will be repulsive if the fullerene is placed on top of the defect's hump, or attractive otherwise, the binding energy is this latter case is 0.06 eV. However, it is important to notice that for relative large room temperature $T = 300$ K these values of the interaction energy are lower than kT, so that the interaction with such defects will not change substantially the main motion of the C_{60} molecule along the nanoribbon.

Our analysis suggests that the C_{60} molecule may create long-lived coupled states with the graphene nanoribbons or graphene sheets of a finite extent, and its sliding along the surface is more energetically favorable than its rocking or rolling. Thus, we may expect that for low temperatures the main type of motion of the fullerene molecules would be sliding, and it will be replaced by rolling at higher temperatures. To verify these ideas, below we provide the numerical modeling of the motion of the fullerene molecules along the graphene surface taking into account all degrees of freedom of the coupled system and considering different values of temperature.

Stochastic motion of C_{60} on a graphene sheet. First, we study the stochastic motion of the fullerene molecule C_{60} placed on a thermalize sheet of graphene. We consider a flat square sheet of graphene of the size 4.1×4.1 nm^2 composed of 678 carbon atoms in the (x, y) plane, as shown in Figs. 4 (a,c). To keep the graphene in the plane, we fix the four edge atoms, shown by solid red circles in the corners of the plots of Figures (a) and (c). We place the molecule C_{60} at the middle of the sheet and place the whole system "buckyball + graphene" consisting of $N = 678 + 60$ atoms into Langevin thermostat modeled by stochastic forces.

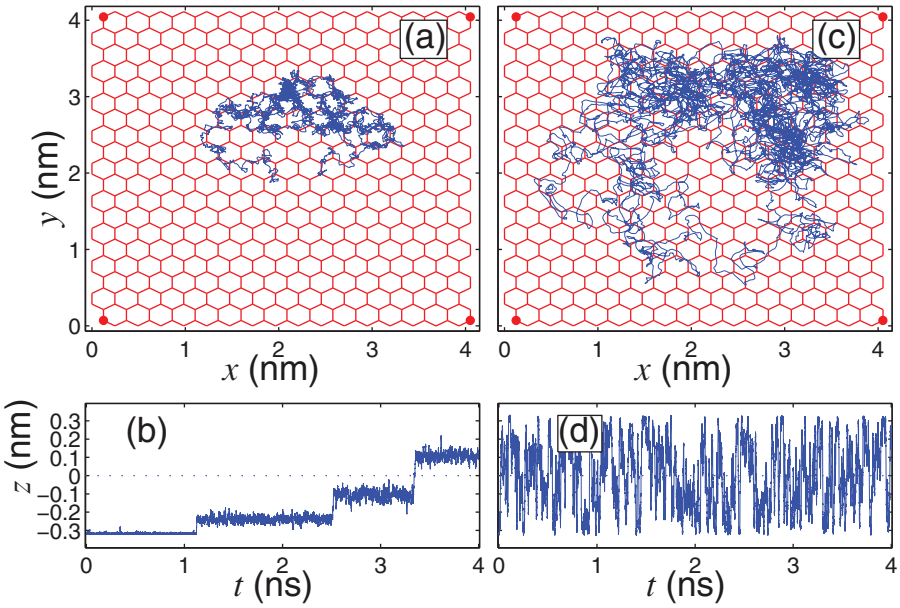

Figure 4 | Stochastic dynamics of the fullerene molecule C_{60} placed on a graphene sheet with the size of 4.1×4.1 nm^2. (a,c) Trajectory of the molecule center shown as a projection on the plane of graphene at the temperatures $T = 30$ K and 300 K, respectively. Red color shows the valent bonds of carbon atoms of the graphene, red dots show the fixed atoms. (b,d) Temporal evolution of the z projection of the center of the hexagonal face relative the molecule's center of mass, for $T = 30$ K and 300 K, respectively.

Our numerical simulations demonstrate that for the temperatures $T \leq 500$ K the molecular system preserves its geometry, namely the buckyball C_{60} remains attached to the graphene sheet, and it undergoes stochastic motion not approaching the edge of the sheet. For very low temperatures $T < 150$ K the main type of motion is sliding along the surface, while for higher temperatures the sliding is replaced by rolling. Figures 4 (a,b) show an example of such a motion at $T = 30$ K when the buckyball moves along the valent bonds of the graphene sheet [see Fig. 4 (a)] changing time to time its sliding face [see Fig. 4 (b)], such that for the time period of 4 ns it changed the face 3 times, as shown in Fig. 4 (b). For higher temperatures such as $T = 300$ K the dynamics is clearly stochastic, and the motion does not reflect much the discrete structure of the graphene substrate, with the contacting face being changed continuously [see Figs. 4 (c,d)]. We observe that in this case the main type of motion is rolling along the graphene sheet, which is energetically more favorable than sliding.

Electorphoresis of $Fe^-@C_{60}$. In order to model numerically the motion of a spherical C_{60} molecule along the graphene nanoribbon under the action of a constant electric field, we include an ion of iron Fe^- into the buckyball, and consider a composite structure $Fe^-@C_{60}$.

We describe the interaction of the iron molecule with the carbon atoms of the molecule C_{60} by employing the LJ potential (5) with the interaction energy $\epsilon_0 = \epsilon_{FeC} = 0.0031$ eV and $\sigma = r_{FeC}/2^{1/6}$, where the equilibrium distance between the atoms is $r_{FeC} = 3.51$ Å. We study the motion of the molecular complex $Fe^-@C_{60}$ along the zigzag nanoribbon consisting of 640 segments with 20 carbon atoms in each. Such a ribbon has the dimensions 157×2 nm^2 and it consists of 12800 carbon atoms [a part of the nanoribbon is shown in Figs. 1 (a–d)].

We place an undeformed nanoribbon in the (x, y) plane along the axes x and fix it in the plane by pinning its four edge atoms. Then, we place the system into the Langevin thermostat by solving numerically the system of stochastic equations (6) with $\Gamma = 1/t_r$, where $t_r = 1$ ps. During the time $t = 10\ t_r$ the system will get thermalized and then we add the molecular complex $Fe^-@C_{60}$. By applying the constant electric field E along the axis x, we create a constant external force $\mathbf{F} = (1, 0, 0)eE$, where e is the electron charge.

Typical dynamics of $Fe^-@C_{60}$ molecule is presented in Fig. 5. Under the action of the electric field the composite molecule moves along the nanoribbon towards its right end not detaching from it. The speed of motion grows monotonously before reaching the maximum velocity v_m. For the field $E = 10^{-7}$ V/m, the maximum velocity $v_m = 390$ m/s which is not sufficient to overtake the effective potential barrier created by the nanoribbon edge, so the molecular complex is reflected from the right end and remains on the nanoribbon, as seen from Fig. 5 (a). However, for higher strength of the external field $E = 2 \times 10^{-7}$ V/m the molecule reaches the maximum velocity $v_m = 540$ m/s, and it may drop off the right end of the nanoribbon. More detailed analysis indicates that the sliding motion is observed only at the beginning of the motion, whereas the main motion of the $Fe^-@C_{60}$ molecule is its rolling along the nanoribbon in the direction of the applied electric field, see Fig. 5 (b).

Thermophoresis of C_{60} molecules. In order to model the motion of a spherical C_{60} molecule under the action of a constant heat flow, we consider the graphene nanoribbon of the size 157×2 nm^2 and place its edges into the Langevin thermostats at different temperatures: first 20 sections – at the temperature $T_+ = 330$ K, and the last 20 sections, at the temperature $T_- = 270$ K. After some transition period, we observe the formation of a constant temperature gradient $dT = 0.30$ K/nm, as shown in Fig. 6 (b). Then, we place a molecule C_{60} on the 22-nd section of the nanoribbon and study its temperature-driven dynamics.

Our modeling demonstrates that C_{60} molecule moves towards the right end of the nanoribbon under the action of the temperature gradient with the constant velocity $v_m = 190$ m/s, see Fig. 6 (a). At the initial stage, the typical motion of the molecule is sliding, but after some time the molecule starts rolling along the nanoribbon, see Fig. 6 (c).

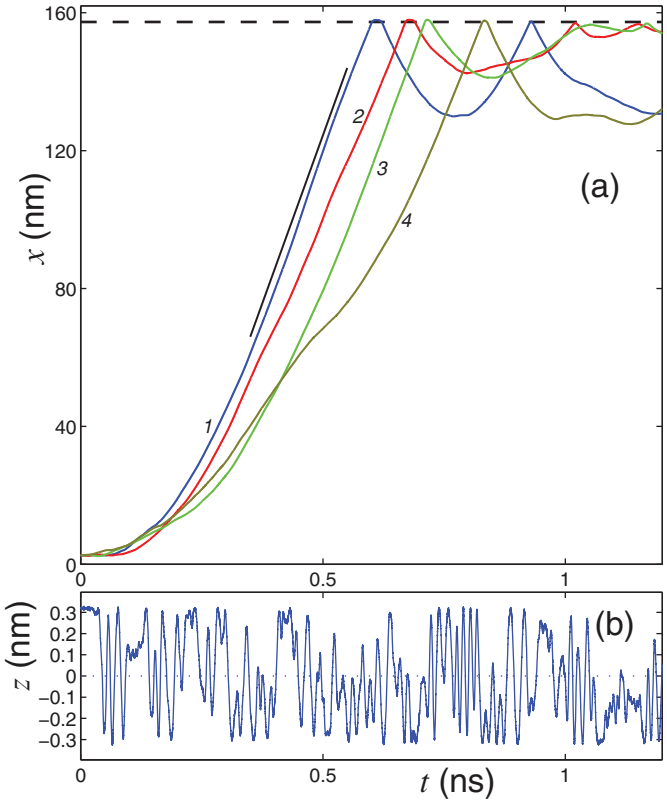

Figure 5 | Transport of the molecular complex Fe−@C60 along the nanoribbon with the dimensions 157×2 nm^2, under the action of the constant electric field $E = 10^{-7}$ V/m, at temperature $T = 300$ K. (a) Evolution of the coordinate of the molecule center for four different thermalization of the nanoribbon (curves 1,2,3, and 4). An auxiliary straight line show the slope of the curves corresponding to the maximum velocity of the molecule, $v_m = 390$ m/s. Dashed straight line marks the location of the edge of the nanoribbon. (b) Temporal evolution of the z projection of the center of the hexagonal face relative the molecule's center of mass, corresponding to the curve 1 in (a).

For larger temperature difference, e.g. $T_+ = 400$ K and $T_- = 200$ K, the temperature gradient is larger, $dT = 0.95$ K/nm [see Fig. 7 (b)], and the molecule speeds up reaching the maximum velocity $v_m = 440$ m/s, and then it, is reflected elastically from the edge of the nanoribbon, see Fig. 7 (a).

Thermophoresis of carbon nanotubes. To compare the transport properties of fullerenes and carbon nanotubes and evaluate the effect of shape on thermophoresis, we consider the mobility of short-length (5,5) carbon nanotubes C_{100}, C_{180} and C_{260}. These nanotubes have the form of short cylinders with the diameter $D = 0.70$ nm (that equals to the diameter of the C_{60} molecule) but with different lengths $L = 1.18$, 2.19 and 3.17 nm, respectively [cf. Figs. 1(a) and (b–d)]. The interaction energy will be maximal provided the nanotube is place along the nanoribbon, so that rocking is hardly possible because for this latter case the nanotube should be placed across the nanoribbon. Therefore, we anticipate that the most typical motion for short-length nanotubes would be their sliding along the surface of the nanoribbon. This is indeed confirmed by our numerical modeling.

Again, we consider the graphene nanoribbon of the size 157×2 nm^2 and place its edges into the Langevin thermostats at different temperatures: first 20 sections – at the temperature $T_+ = 400$ K, and the last 20 sections, at the temperature $T_- = 200$ K. After some

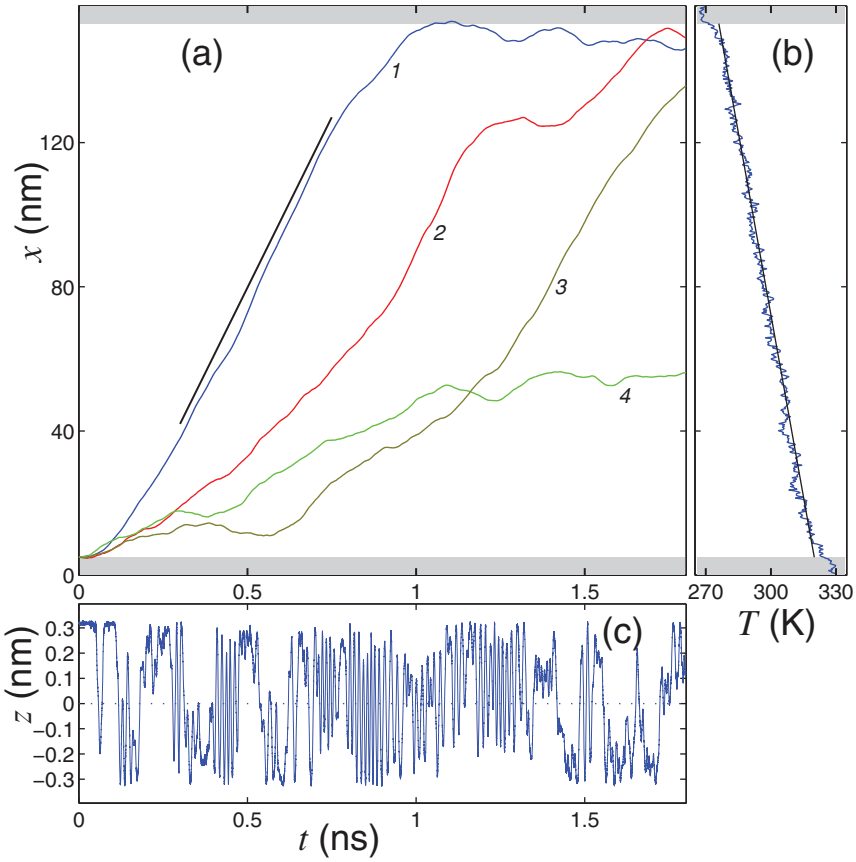

Figure 6 | Transport of the C_{60} molecule along the nanoribbon with the size 157 × 2 nm², under the action of a heat flow. (a) Evolution of the coordinate of the molecule center for four different scenarios of thermalization of the nanoribbon (curves 1,2,3, and 4). An auxiliary straight line shows the slope of the curves corresponding to the maximum velocity of the molecule, $v_m = 190$ m/s. (b) Temperature profile along the nanoribbon, a solid straight line corresponds to the temperature gradient of $dT = 0.30$ K/nm. Grey shaded areas show the edge areas of the nanoribbon subjected to two Langevin thermostats at $T_+ = 330$ K and $T_- = 270$ K, respectively. (c) Temporal evolution of the z projection of the center of the hexagonal face relative the molecule's center of mass, corresponding to the curve 1 in (a).

transition period, we observe the formation of a constant temperature gradient $dT = 0.95$ K/nm, as shown in Fig. 7 (b). Then, we place a nanotube next to the left end of the nanoribbon and study its temperature-driven dynamics.

Our modeling demonstrates that the nanotube moves towards the right end of the nanoribbon under the action of the temperature gradient with the constant velocity v_m, see Fig. 7 (a). The maximum velocities are: $v_m = 444$ m/s, for C_{60} molecule, and $v_m = 396, 328$ and 283 m/s, for the nanotubes C_{100}, C_{180}, and C_{260}, respectively. Moreover, our study indicates that the nanotubes do not roll but instead they slide along the surface, this is indicated by the study of the temporal evolution of the z projection of the center of the pentagonal face relative the nanotube's center of mass, as shown in Fig. 7 (c).

Discussion

We have studied the motion of fullerene molecules and short-length carbon nanotubes along the deformable surface of a graphene nanoribbon in several cases, including the stochastic motion and directed motion in the presence of an electric field or a thermal gradient. We have revealed that the mobility of carbon structures depends substantially on their shape and symmetry, so that larger molecules and more asymmetric structures demonstrate much lower mobility than C_{60} molecules. We have demonstrated that both electorphoresis and thermophoresis can be employed to control the transport of carbon structures and fullerenes through their shape, size, and possible inclusions. Thus, our analysis indicates that long graphene nanoribbons may play a role of conveyor belts for the transportation of the fullerene molecules and short nanotubes.

Methods

The first study of the van der Waals (VDW) energy for the interaction of fullerene molecule C_{60} and substrate with atomic surface corrugation was presented in Ref. 19. The VDW energy was calculated using linear response theory to evaluate the dipole-dipole interactions between the molecule and the substrate. Interaction of the fullerene C_{60} with graphite surface was described by the 12-6 Lennard-Jones (LJ) potential

$$V(r) = C_{12}/r^{12} - C_6/r^6 \quad (1)$$

with the coefficients $C_{12} = 12000$ eVÅ^{12} and $C_6 = 15.2$ eVÅ^6.

Experimental evaluation of the interaction of molecule C_{60} with single-wall carbon nanotubes (SWNTs) and graphite was obtained in Ref. 18, on the basis of the thermal desorption spectroscopy. It was shown that these interactions can be modeled, with a high accuracy, by the LJ potential (1) with coefficients $C_{12} = 22500$ eVÅ^{12} and $C_6 = 15.4$ eVÅ^6. This potential has been employed for the modeling absorption of C_{60} molecules by single-walled carbon nanotubes with open ends.

Inside of the fullerene molecule and a sheet of graphene the molecules two neighboring carbon atoms create a valent bond [see Fig. 8 (a)]. We describe the energy associated with the deformation of the valent bond created by two carbon atoms by the following interaction potential

$$U_1(\rho) = \epsilon_1\{\exp[-\alpha(\rho-\rho_1)]-1\}^2, \quad (2)$$

where ρ is the length of the valent bond, $\epsilon_1 = 4.9632$ eV and $\rho_1 = 1.418$ Å is the energy and the equilibrium length of the bond, parameter $\alpha = 1.7889$ Å^{-1}. Each carbon atom is placed at the vertex of three planar valent angles. The corresponding deformation energy of a plane valent angle created by three atoms [see Fig. 8 (b)] can be described by the interaction potential of the form,

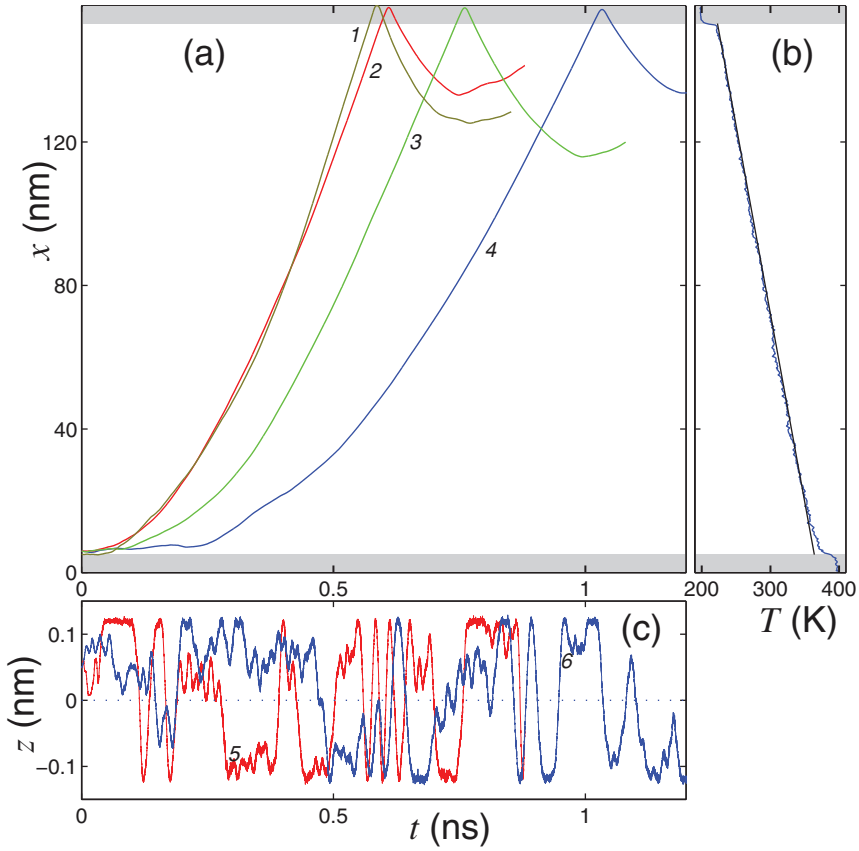

Figure 7 | (a) Transport of the spherical C_{60} molecule, and three different short-length (5,5) carbon nanotubes C_{100}, C_{180} and C_{260} along the zigzag nanoribbon of the size 157×2 nm^2 under the action of a heat flow. Shown is the evolution of the coordinate of the molecule center for four cases (curves 1, 2, 3 and 4, respectively). (b) Temperature profile along the nanoribbon, a solid straight line corresponds to the temperature gradient of $dT = 0.95$ K/nm. Grey shaded areas show the edge areas of the nanoribbon subjected to two Langevin thermostats at $T_+ = 400$ K and $T_- = 200$ K, respectively. (c) Temporal evolution of the z projection of the center of the pentagonal face relative the molecule's center of mass, corresponding to the curves 2 and 4 in (a).

$$U_2(\varphi) = \epsilon_2(\cos\varphi + 1/2)^2, \tag{3}$$

where φ is value of the valent angle (equilibrium value of the angle $\varphi = 2\pi/3$), energy $\epsilon_2 = 1.3143$ eV. Each valent bond is simultaneously belong to two planes, so that the deformation energy of the angle formed by two such planes can be described by the following interaction potential,

$$U_i(\phi) = \epsilon_i(1 - \cos\phi), \tag{4}$$

where ϕ – is the corresponding angle (in equilibrium, $\phi = 0$), and the index $i = 3, 4, 5$ describe the type of the dihedral angle – see Fig. 8 (c), (d), (e). Energy $\epsilon_3 = \epsilon_4 = 0.499$ eV, $\epsilon_5 \ll \epsilon_4$, so that the latter contribution to the total energy can be neglected.

More detailed discussion and motivation of our choice of the interaction potentials (2), (3), (4) can be found in Ref. 20. Such potentials have been employed for modeling of thermal conductivity of carbon nanotubes[21,22] graphene nanoribbons[20] and also in the analysis of their oscillatory modes[23–25]. In particular, in Ref. 22 a detailed comparison of the results obtained with the help of the potential used in this paper with the results obtained with the help of Brener potential was presented. It was shown that numerical modeling of carbon nanotubes demonstrate similar results for both the potentials, however the potential used here allows calculating the frequency spectra with higher accuracy, as compared with the experimental data.

We describe the nonvalent interaction of carbon atoms belonging to the fullerene molecule and graphene by the Lennard-Jones 12-6 potential

$$U_{LJ}(r) = 4\epsilon_0\left[\left(\frac{\sigma}{r}\right)^{12} - \left(\frac{\sigma}{r}\right)^{6}\right], \tag{5}$$

where r – distance between the atom centers, interaction energy $\epsilon_0 = \epsilon_{CC} = 0.002635$ eV, and parameter $\sigma = \sigma_{CC} = 3.3686$ Å. Potential (5) coincides with the potential (1) for the coefficients $C_{12} = 4\epsilon_{CC}\sigma_{CC}^{12} = 22500$ eV/A^{12}, $C_6 = 4\epsilon_{CC}\sigma_{CC}^{6} = 15.4$ eV/A^6 (see[18]).

The motion equations for molecular complex "fullerene + graphene" are taken in the form

$$M_i\ddot{\mathbf{u}}_i = -\frac{\partial H}{\partial \mathrm{u}_i} - \Gamma M_i\dot{\mathbf{u}}_i + \Xi_i, \tag{6}$$

where H is Hamiltonian of the complex, the indices $i = 1, 2, \ldots, N$ stand for the atom number, the vector $\mathbf{u}_i = (u_{i,1}, u_{i,2}, u_{i,3})$ describes the position of the atom, and M_i is the atom mass. Langevin collision frequency is $\Gamma = 1/t_r$, where t_r – particle relaxation time, and $\Xi_i = (\xi_{i,1}, \xi_{i,2}, \xi_{i,3})$ is a three-dimensional vector of Gaussian stochastic forces describing the interaction of the i-th atom with thermostat.

We consider a hydrogen-terminated graphene, where all edge atoms correspond to the CH group. In our model, we treat such a group as a single effective particle at the

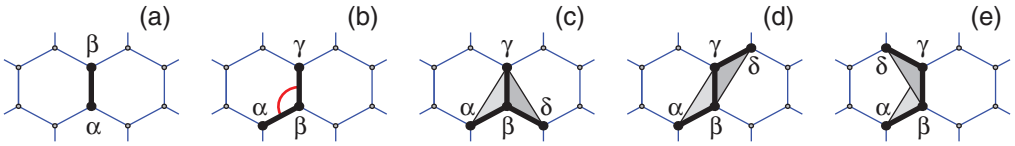

Figure 8 | **Typical configurations of the nanoribbon bonds containing up to i-th nearest-neighbor interactions for: (a) $i = 1$, (b) $i = 2$, (c) $i = 3$, (d) $i = 4$, and (e) $i = 5$.**

location of the carbon atom, so that we take the mass of atoms inside the graphene sheet and fullerene atoms as $M_i = 12\ m_p$, but for the atoms at the graphene edge we consider an effective particle with a larger mass $M_i = 13\ m_p$ (where $m_p = 1.6603 \times 10^{-27}$ kg is the proton mass).

To analyze the thermalized dynamics of the system, we introduce a random white noise with the correlation functions

$$\left\langle \xi_{i,k}(t_1)\xi_{j,l}(t_2)\right\rangle = 2M_i\Gamma k_B T\delta_{ij}\delta_{kl}\delta(t_2-t_1), \qquad i,j=1,2,\ldots,N,\quad k,l=1,2,3, \tag{7}$$

where T is the temperature of the Langevin thermostat. We select relatively large relaxation time $t_r = 1$ ps to reduce the effect of viscosity in the molecular dynamics, and integrate the system of equations (6) for the time interval $t = 4$ ns (for the period $t = 10\ t_r = 10$ ps the system should relax into the equilibrium state with the thermostat and then it will evolve as a fully thermalized system).

1. Drexler, K. E. *Nanosystems: Molecular Machinery, Manufacturing, and Computation* (New York, Wiley, 1992).
2. Novoselov, K. S., Geim, A. K., Morozov, S. V., Jiang, D., Zhang, Y., Dubonos, S. V., Grigorieva, I. V. & Firsov, A. A. Electric Field Effect in Atomically Thin Carbon Films. *Science* **306**, 666–669 (2004).
3. Geim, A. K. & MacDonald, A. H. Graphene: Exploring Carbon Flatland. *Phys. Today* **60**, 35 (2007).
4. Castro Neto, A. H., Guinea, F., Peres, N. M., Novoselov, K. S. & Geim, A. K. The electronic properties of graphene. *Rev. Mod. Phys.* **81**, 109–162 (2009).
5. Meyer, J. C., Girit, C. O., Crommie, M. F. & Zettl, A. Imaging and dynamics of light atoms and molecules on graphene. *Nature* **454**, 319 (2008).
6. Barreiro, A., Rurali, R., Hernandez, E. R., Moser, J., Pichler, T., Forro, L. & Bachtold, A. Subnanometer Motion of Cargoes Driven by Thermal Gradients Along Carbon Nanotubes. *Science* **320**, 775–778 (2008).
7. Neek-Amal, M. & Lajevardipour, A. Stochastic motion of noble gases on a graphene sheet. *Comp. Mat. Sci.* **49**, 839 (2010).
8. Neek-Amal, M., Abedpour, N., Rasuli, S. N., Naji, A. & Ejtehadi, M. R. Diffusive motion of C_{60} on a graphene sheet. *Phys. Rev. E* **82**, 051605 (2010).
9. Itamura, N., Asawa, H., Miura, K. & Sasaki, N. Unique Near-Zero Friction Regime of C_{60} Molecular Bearings Along [12$\bar{3}$0. Direction. *J. Phys.: Conference Series* **258**, 012013 (2010).
10. Lohrasebi, A., Neek-Amal, M. & Ejtehadi, M. R. Directed motion of C_{60} on a graphene sheet subjected to a temperature gradient. *Phys. Rev. E* **83**, 042601 (2011).
11. Golo, V. L., Salnikov, Vl. N. & Shaitan, K. V. Harmonic oscillators in the Nose-Hoover environment. *Phys. Rev. E* **70**, 046130 (2004).
12. Legoll, F., Luskin, M. & Moeckel, R. Non-ergodicity of Nosé-Hoover dynamics. *Nonlinearity* **22**, 1673 (2009).
13. Ishikawa, M., Kamiya, S., Yoshimoto, S., Suzuki, M., Kuwahara, D., Sasaki, N. & Miura, K. Nanocomposite Materials of Alternately Stacked C_{60} Monolayer and Graphene. *J. Nanomaterials* **2010**, 891514 (2010).
14. Xue, Y. & Chen, M. Dynamics of molecules translocating through carbon nantubes as nanofluidic channels. *Nanotechnology* **17**, 5216 (2006).
15. Su, H., Goddard III, W. A. & Zhao, Y. Dynamic friction force in a carbon peapod oscillator. *Nanotechnology* **17**, 5691 (2006).
16. Hai-Yang, S. & Xin-Wei, Z. Molecular dynamics study of effects of radius and defect on oscillatory behaviors of C60- nanotube oscillators. *Phys. Lett. A* **373**, 1058 (2009).
17. Rurali, R. & Hernandez, E. R. Thermally induced directed motion of fullerene clusters encapsulated in carbon nanotubes. *Chem. Phys. Lett.* **497**, 62 (2010).
18. Ulbricht, H., Moos, G. & Hertel, T. Interaction of C_{60} with carbon nanotubes and graphite. *Phys. Rev. Lett.* **90**, 095501 (2003).
19. Gravil, P. A., Devel, M., Lambin, Ph., Bouju, X., Girard, Ch. & Lucas, A. A. Adsorption of C60 molecules. *Phys. Rev B* **53**, 1622 (1996).
20. Savin, A. V., Kivshar Yu, S. & Hu, B. Suppression of thermal conductivity in graphene nanoribbons with rough edges. *Phys. Rev. B* **82**, 195422 (2010).
21. Savin, A. V., Kivshar Yu, S. & Hu, B. Effect of substrate on thermal conductivity of single-walled carbon nanotubes. *Europhys. Lett.* **88**, 26004 (2009).
22. Savin, A. V., Hu, B. & Kivshar Yu, S. Thermal conductivity of single-walled carbon nanotubes. *Phys. Rev. B* **80**, 195423 (2009).
23. Savin, A. V. & Kivshar Yu, S. Localized modes in capped single-walled carbon nanotubes. *Appl. Phys. Lett.* **94**, 111903 (2009).
24. Savin, A. V. & Kivshar Yu, S. Surface solitons at the edges of graphene nanoribbons. *Europhys. Lett.* **89**, 46001 (2010).
25. Savin, A. V. & Kivshar Yu, S. Vibrational Tamm states at the edges of graphene nanoribbons. *Phys. Rev. B* **81**, 165418 (2010).

Acknowledgements

Alex Savin acknowledges a warm hospitality of the Nonlinear Physics Center at the Australian National University, and he thanks the Joint Supercomputer Center of the Russian Academy of Sciences for the use of their computer facilities. The work was supported by the Australian Research Council.

Author contributions

Alex Savin was engaged in modeling and numerical simulations, and both the authors contributed equally into discussions and writing the paper.

Additional information

Competing financial interests: The authors declare no competing financial interests.

How to cite this article: Savin, A.V. & Kivshar, Y.S. Transport of fullerene molecules along graphene nanoribbons. *Sci. Rep.* **2**, 1012; DOI:10.1038/srep01012 (2012).